TABLE V

ELECTRICAL RESISTIVITIES (μOHM CM.)

	$K_{0.40}WO_3$		$Rb_{0.32}WO_3$	
T, °K.	Computed	Obsd.	Computed	Obsd.
0	6.9	...	10.0	...
50	6.9	...	10.0	...
100	8.2	...	12.2	...
150	13.4	12.8	21.1	20.6
200	21.0	21.4	34.1	34.8
250	29.4	29.6	48.6	49.2
300	37.9	38.2	63.0	64.0
350	46.1	46.8	77.0	78.4
400	54.7	...	91.7	...

TABLE VI

MAGNETIC PARAMETERS OF K AND Rb TUNGSTEN BRONZES

Composition	$\chi_{dia} \times 10^6$ correction	$\kappa_{e^-} \times 10^6$ exptl.	$n \times 10^{-21}$, e^-/cc.	$\kappa_{e^-} \times 10^6$ theor.	m^*/m_0
$Rb_{0.26}WO_3$	−18.7	0.49	4.4	0.24	1.6
$K_{0.23}WO_3$	−16.3	.21	3.8	.23	0.9
$K_{0.29}WO_3$	−17.2	.35	4.7	.25	1.2
$K_{0.30}WO_3$	−17.4	.35	4.9	.25	1.2
$K_{0.45}WO_3$	−17.6	1.3	7.8	.29	2.9

can be explained by having a delocalized spin system as would exist in a conduction band. In such a case, the magnetic susceptibility can be computed from the quasi-free-electron model following the procedure of Sienko and Truong.[13] Table VI summarizes the parameters involved in the computation, assuming diamagnetic contributions[29] of -14.6×10^{-6} per mole of K^+, -22.0×10^{-6} per mole of Rb^+, and -13.0×10^{-6} per mole of WO_3. (The correction for WO_3 was determined by actual measurement on the Fisher "purified tungstic anhydride" from which the bronzes were prepared. As also found by Greiner, Shanks, and Wallace,[28] this material is less diamagnetic than the -21.0×10^{-6} value reported by Conroy and Sienko. The latter was based on measurements made on WO_3 samples which were carefully purified by multiple reprecipitation techniques.)

As given in the table, κ_{e^-} experimental is the observed magnetic susceptibility per unit volume attributable to the electrons. It is computed by subtracting the appropriate diamagnetic corrections for M^+ and WO_3 from the observed susceptibility and dividing the difference by the molar volume of the bronze. The values given for κ_{e^-} theoretical are computed from the Pauli–Peierls equation[30]

$$\kappa_{e^-} = \frac{4m^*\mu_0^2}{h^2}(3\pi^2 n)^{1/3}\left(1 - \frac{m_0^2}{3m^{*2}}\right)$$

using the assumption that the conduction electrons are completely free—that is, that the effective mass of the electrons, m^*, is equal to the electronic rest mass, m_0. To reconcile the observed electronic susceptibility with the theoretical, it is necessary to assume that the effective mass of the carriers is greater than the rest mass by the amounts shown in the last column of Table VI. Except for the last entry, for $K_{0.45}WO_3$, the effective masses for the K and Rb tungsten bronzes closely approximate the values characteristic of the Li and Na tungsten bronzes, in spite of the anisotropic character of the former. The unusually high effective mass in $K_{0.45}WO_3$ agrees with the higher susceptibility of $K_{0.53}WO_3$ previously reported by Kupka and Sienko. The break in Table VI between the last and the next-to-last lines coincides with the division between tetragonal and hexagonal structures.

The need for further single crystal work to examine any anisotropy in both the conductivity and the magnetic susceptibility is clearly evident. However, the general model for tungsten bronzes in which M interstitials are assumed to have donated electrons to a conduction band of the host WO_3 seems to be substantially supported by the above work.

---

(29) G. W. Brindley and F. E. Hoare, *Trans. Faraday Soc.*, **33**, 268 (1937); *Proc. Phys. Soc.* (London), **49**, 619 (1937).

(30) See, for example, A. H. Wilson, "The Theory of Metals," 2nd Ed., Cambridge University Press, Cambridge, 1954, p. 155.

CONTRIBUTION FROM THE CHEMISTRY DEPARTMENT,
UNIVERSITY OF MICHIGAN, ANN ARBOR, MICHIGAN

Oxidation of Thin Single Crystals of Copper[1]

BY R. B. MARCUS AND L. O. BROCKWAY

Received December 10, 1962

Single crystal films of copper of 700–800 Å. thickness have been prepared in two states: (a) showing many wide stacking faults and few dislocations, and (b) showing no stacking faults and a high density of dislocations. On treatment with oxygen gas at 0.9 μ and 525° cuprous oxide crystals appear with two epitaxial relations to the copper. On the type (a) copper film the oxide particles show some tendency to nucleate along the stacking faults. On both types the oxide growth has a 20-min. incubation period followed by the sudden appearance of oxide grains of 0.5 μ diameter which increase in size by twofold in the following 20 min.

Chemical reactions involving a solid phase as one of the reactants are probably as old as chemistry itself, but only quite recently have the techniques been developed which allow the detailed study of the influence of the physical state of the solid on its chemical behavior. With the techniques of electron microscopy and electron

---

(1) This work was supported in part by the Atomic Energy Commission under Contract No. AT(11-1)-1086.

diffraction now available it is possible to obtain information both on the imperfections in the structure of the solid reactant and on the nature of the reaction product on its surface during the very early stages of the reaction. Information on the reaction product may include not only the identity and rate of formation but also observations on the sites of nucleation, the epitaxial relations between the crystalline product and the substrate, and on the sizes and shapes of the particles of product. For such studies a single crystal as the solid reactant affords the possibility of a more precise description of the reactant and of events on the surface than a polycrystalline or amorphous substance does. Of particular interest is the question of the influence of dislocations and stacking faults in the solid reactant on its chemical properties. The reaction considered here is the oxidation of crystalline copper with oxygen gas.

Previous observations on the oxidation of copper single crystals have involved specimens of about 1 cm. in thickness. Benard[2] and co-workers oxidized bulk single crystals of copper under conditions of varying pressure and temperature and made observations using optical microscopy on the dependence of epitaxy and texture of Cu_2O on oxidation temperature and pressure. Lawless and Gwathmey[3] made similar observations on bulk crystals, using the electron microscope to study replicas of oxidized surfaces. Harris,[4] using a technique of removing the oxide film and direct examination of the oxide by electron microscopy and electron diffraction, showed that at least three different textures of Cu_2O were present at any one time during the early period of oxidation: a continuous basal film, small nuclei (~20–80 Å.), and larger "polyhedra" (~2000 Å.). He found some difference in the number and rate of growth of polyhedra depending upon the stress history of the copper crystal, indicating a possible influence on oxidation of stress-induced dislocations in the copper. Using a replica technique on oxidized bulk crystals, Young[5] was able to show a correlation between the number of Cu_2O nuclei per unit surface area of copper and the density of dislocations for the case of copper that had been "doped" with 0.05 atom % of tin or 0.01 atom % of tellurium.

In the present experiment, high purity copper in the form of a thin (700–800 Å.) single crystal is oxidized by oxygen gas at a pressure of 0.9 μ and at 525°. The metal crystal is thin enough that it can be examined directly by transmission in an electron microscope and its structural imperfections observed. After treatment with oxygen the oxide formed can be observed in place on the metal so that any correlation between the sites of oxidation and the positions of imperfections in the substrate and also the relative crystallographic orientations are evident.

The thin copper crystals are prepared by a method which allows some control over the extent and density of stacking faults and dislocations. High purity copper (99.999%) is condensed from the vapor onto a single crystal of sodium chloride at 330°. The residual pressure during the copper evaporation is less than 1×10^{-5} mm., and the deposition rate is 330 Å/min. The copper subsequently is annealed at 630° in hydrogen at a pressure of 1 atm. and a flow rate of 1.2 cc./sec. for 10 min., either before its removal from the sodium chloride substrate or after it has been lifted off and mounted on electron microscope specimen grids. In either case the copper film is a single crystal extended in the (001) plane, but the films annealed on the sodium chloride show a high concentration (averaging 0.5×10^4 cm.^{2}/cm.^{3} of copper) of wide stacking faults (averaging 2×10^{-4} cm. in width) and low density of dislocations as shown in Fig. 1. The films annealed after removal from the sodium chloride show almost no stacking faults and a high density of dislocations (approximately 10^9/cm.^{2}). The characteristics of these crystals are more fully described elsewhere.[6]

Such films mounted on microscope specimen grids of gold or copper were oxidized in purified oxygen gas at various pressures and temperatures: the results shown here were obtained at oxygen pressures of 0.9 μ and a temperature of 525° with oxidation times ranging from 5–45 min.

Representative micrographs of the oxidized copper films of the two kinds are shown in Fig. 2 and 3. The grains of about 1 μ diameter are cuprous oxide, the only oxidation product observed. The electron diffraction patterns with which the oxide was identified also show that it consists almost entirely of distinct single crystals aligned on the copper within 5° of two orientations: the predominant orientation is Cu_2O (001)||Cu (001) and Cu_2O [100]||Cu [100], and the secondary orientation shows Cu_2O (111)||Cu (001) with Cu_2O $[1\bar{1}0]$||Cu $[1\bar{1}0]$ or Cu_2O $[1\bar{1}0]$||Cu [110].

The oxidation reaction shows an incubation period of 20 min. which is followed by the sudden appearance of a number of oxide grains.[7] Both at the initial appearance of oxide and during the later oxidation the oxide grains on any one film are remarkably uniform in size. Grains smaller than about 0.5 μ have not been observed although the size does increase above 1 μ with the longer oxidation times. Evidently the nucleation of oxide occurs only during a very short period at the close of the incubation period and the growth of the nuclei must be very rapid at first. The incubation period can be shortened by heating the hydrogen-annealed copper crystal to the 525° temperature under vacuum before introducing the oxygen gas; the presumption is that hydrogen dissolved in the copper diffuses away and no longer interferes with the subsequent reaction with oxygen. The occurrence of an incubation period also has been noted by Benard,

---

(2) J. Benard, F. Gronlund, J. Oudar, and M. Duret, *Z. Elektrochem.*, **63**, 799 (1959).

(3) K. R. Lawless and A. T. Gwathmey, *Acta Met.*, **4**, 153 (1956).

(4) W. W. Harris, F. Ball, and A. T. Gwathmey, *ibid.*, **5**, 574 (1957).

(5) F. W. Young, *ibid.*, **8**, 117 (1960).

(6) L. O. Brockway and R. B. Marcus, *J. Appl. Phys.*, submitted for publication.

(7) Note Added in Proof.—Subsequent experiments show that the 20 min. incubation period is not reproducible but varies down to about 3 min.

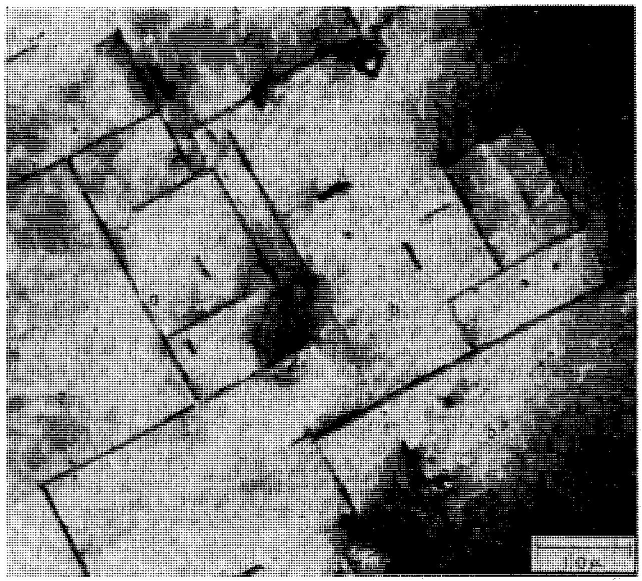

Fig. 1.—Copper film annealed on sodium chloride, showing stacking faults at a and dislocations at b.

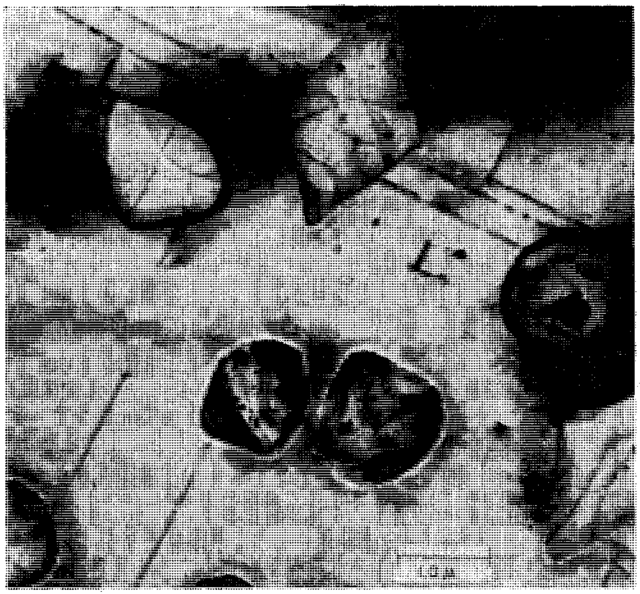

Fig. 2.—Copper film oxidized at 525° for 35 min.; this film was annealed in H_2 on sodium chloride prior to oxidation.

et al.,[2] who reported observations in optical micrographs on the oxidation of thick specimens of copper.

The 1 μ lateral dimension of the oxide grains is about ten times the original thickness of the metal film. The grains lie in or above holes in the copper as shown by the holes observed after treatment of the oxidized film with dilute hydrochloric acid, which dissolves the cuprous oxide without appreciable attack on the copper. This position of the oxide grains would account for the more rapid initial rate of growth when the original nucleus on the surface of the film is in contact with copper through a solid angle of 2π; when all of the copper lying under the nucleus has been oxidized the total interfacial area between the copper and oxide is greatly reduced and the growth rate is much slower.

The observations just described are generally similar for the two types of copper films, but differences do occur in the density and location of the oxide grains. On the films showing stacking faults the density of oxide grains is about 10^7/cm.^{2} of copper surface (Fig. 2). The oxide grains observed in these experiments often are larger than the separation between stacking faults; when the grains are smaller there is a significant tendency to be located on or very close to the stacking faults, as shown in Fig. 4. On films annealed after removal from sodium chloride the surface density of oxide grains tends to be greater than on the other type of copper film, ranging up to 3 × 10^7/cm.^{2}.

Carbon replicas of the unoxidized films with stacking

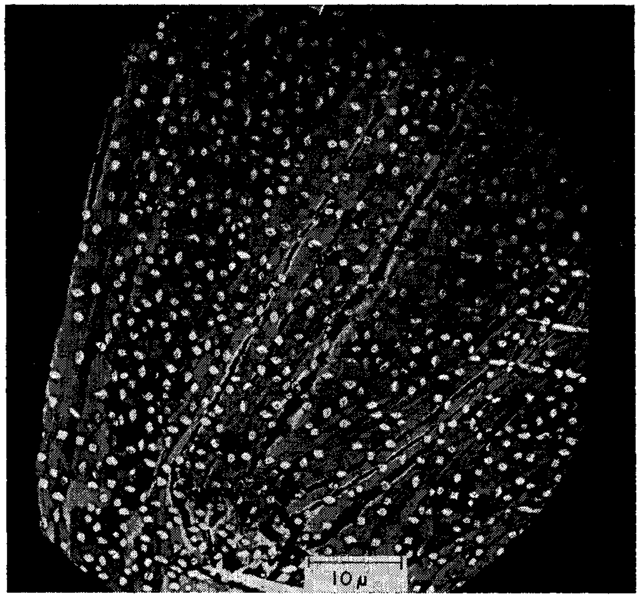

Fig. 3.—Copper film oxidized at 525° for 22 min.; this film was annealed in H_2 on microscope specimen grids prior to oxidation.

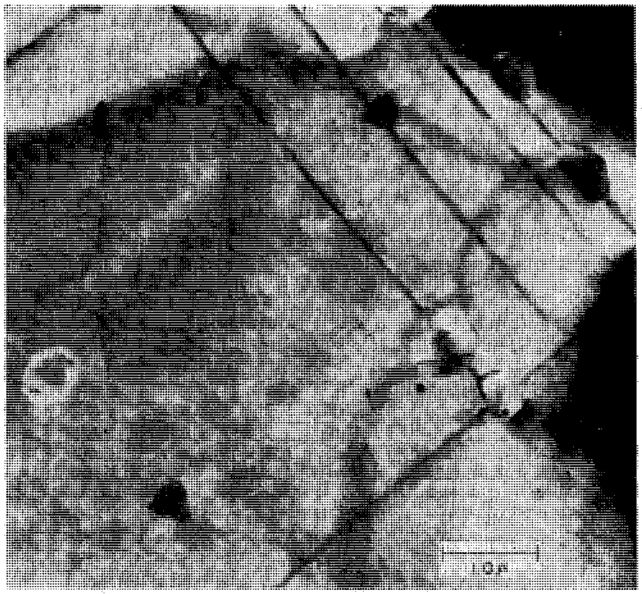

Fig. 4.—Copper film oxidized at 525° for 21 min.; this film was annealed in H_2 on sodium chloride prior to oxidation. There is a significant tendency for oxide grains to be located in the vicinity of stacking faults.

faults indicate terraces of about 50–100 Å. in height in the surface of the film where the stacking fault reaches the surface. It is suggested that the preferential nucleation for oxide formation at stacking faults involves the first appearance of oxide either at the reentrant angle or the external angle of the terrace stepsite. On films annealed on specimen grids and not showing stacking faults, the variation in surface density of oxide grains often is correlated with extinction contour patterns in micrographs of these films, suggesting a relationship between elastic strain in the copper and nucleation of oxide grains.

In this work we have observed a definite indication of influence of the physical state of the copper on the number and location of sites which are active for the formation of cuprous oxide. The investigation is being extended to provide data for a statistical survey and to include oxidation of copper films where the physical state is altered by thermal stresses, by direct mechanical stresses, and by the incorporation of impurity atoms.

CONTRIBUTION FROM THE CHEMISTRY DIVISION,
ARGONNE NATIONAL LABORATORY, ARGONNE, ILLINOIS

Uranium–Oxygen Bond Lengths in Uranyl Salts: Uranyl Fluoride and Uranyl Carbonate[1]

BY HENRY R. HOEKSTRA

Received September 28, 1962

Infrared absorption curves for carefully purified samples of UO_2F_2 and UO_2CO_3 have been obtained. Using the new frequencies and Badger's rule, the uranyl bond lengths are calculated as 1.71 Å. in UO_2F_2 and 1.72 Å. in UO_2CO_3, in very good agreement with the Zachariasen bond length–bond strength relationship. Evidence is given to show that the U–O bond length in different uranyl salts shows relatively little variation (1.71–1.76 Å.) and that the bond order in the simple anhydrous salts may approach three.

Introduction

The uranium coördination sphere in hexavalent uranium compounds is generally unsymmetrical, consisting of two short strong bonds to oxygen atoms situated above and below the central uranium atom and four, five, or six longer bonds distributed in or near a plane normal to the uranyl axis.[2] At present it is generally conceded that the O–U–O entity, the uranyl group, is linear in the solid state, and probably in solution, as well.

Unfortunately, the poor X-ray diffracting power of oxygen as compared with uranium leads to difficulties in locating the uranyl oxygen atoms with any degree of precision. In general, single crystal X-ray or neutron diffraction studies are required to provide accurate bond lengths. The good structural data which do exist clearly indicate that the uranyl bond length is not constant in the various U(VI) compounds.

Based on his X-ray studies of a number of U(VI) compounds, Zachariasen[2] was able to show that a single curve can be drawn to relate the uranium–oxygen bond length to its bond strength. This relationship applies to the equatorial, or secondary, oxygen atoms as well as to the uranyl, or primary, oxygen atoms. The total bond strength, as used by Zachariasen, is obtained by assuming that each atom has a bonding capability as given by its valence in the compound and that this bond strength sum is distributed over all the bonds formed by that atom. The strength of each bond varies inversely with the bond length. A subsequent publication[3] provides some minor revisions in the bond length curve.

The empirical bond length–bond strength relationship has been found to give good agreement with accurate bond length measurements as they have become available and has been utilized by others to estimate uranyl bond lengths where they could not be measured accurately.

Jones[4] has investigated the feasibility of determining the bond lengths by infrared techniques. The uranyl ion exhibits three characteristic vibrational frequencies: the symmetric (ν_1) and asymmetric (ν_3) stretching vibrations and the bending (ν_2) vibration. Of these three, only the asymmetric frequency is generally observed, since the symmetric vibration should be infrared inactive for a linear UO_2^{+2} ion, and the bending frequency lies outside the range of most infrared instruments. The location of ν_1 can sometimes be determined by observation of the $\nu_1 + \nu_3$ combination frequency. Accepted location for the vibrations are $\nu_1 \cong 860$ cm.$^{-1}$, $\nu_3 \cong 930$ cm.$^{-1}$, and $\nu_2 \cong 200$ cm.$^{-1}$, although ν_1 and ν_3 are known to appear over a substantial frequency range extending from approximately 800 to 1000 cm.$^{-1}$.

Jones pointed out that application of Badger's[5] relationship (1) to force constants calculated from infrared spectra permits an evaluation of the uranyl bond length

$$R_{UO} = \beta F_{UO}^{-1/3} + d_{UO} \qquad (1)$$

---

(1) Base on work performed under the auspices of the U. S. Atomic Energy Commission.

(2) W. H. Zachariasen, *Acta Cryst.*, **7**, 795 (1954).

(3) W. H. Zachariasen and H. A. Plettinger, *ibid.*, **12**, 526 (1959).

(4) L. H. Jones, *Spectrochim. Acta*, **10**, 395 (1958); *ibid.*, **11**, 409 (1958).

(5) R. M. Badger, *J. Chem. Phys.*, **2**, 128 (1934); **3**, 710 (1935).